JOURNAL OF THEORETICAL AND APPLIED MECHANICS
44, 3, pp. 603-636, Warsaw 2006

EVALUATION OF FRACTURE PARAMETERS FOR CRACK PROBLEMS IN FGM BY A MESHLESS METHOD

Jan Sladek
Vladimir Sladek

Institute of Construction and Architecture, Slovak Academy of Sciences, Bratislava, Slovakia
e-mail: usarslad@savba.sk

Chuanzeng Zhang

Department of Civil Engineering, University of Siegen, Germany

Choon-Lai Tan

Department of Mechanical and Aerospace Engineering, Carleton University, Ottawa, Canada

A meshless method based on the local Petrov-Galerkin approach is proposed for crack analysis in two-dimensional (2D), anisotropic and linear elastic solids with continuously varying material properties. Both quasi-static thermal and transient elastodynamic problems are considered. For time-dependent problems, the Laplace transform technique is utilized. The analyzed domain is divided into small subdomains of circular shapes. A unit step function is used as the test function in the local weak form. It leads to Local Integral Equations (LIE) involving a domain-integral only in the case of transient dynamic problems. The Moving Least Squares (MLS) method is adopted for approximating the physical quantities in the LIE. Efficient numerical methods are presented to compute the fracture parameters, namely, the stress intensity factors and the T-stress, for a crack in Functionally Graded Materials (FGM). The path-independent integral representations for stress intensity factors and T-stresses in continuously non-homogeneous FGM are presented.

Key words: stress intensity factors, T-stress, meshless methods, thermoelasticity, nonhomogenity, orthotropic materials

1. Introduction

Functionally Graded Materials (FGM) possess continuously nonhomogeneous material properties. These materials have been introduced in recent years to

benefit from the ideal performance of their constituents, e.g. high heat and corrosion resistances of ceramics on one side, and large mechanical strength and toughness of metals on the other side. In FGM, the composition and the volume fraction of their constituents vary continuously with spatial coordinates. A review on various aspects of FGM can be found in the monograph by Suresh and Mortensen (1998) and the review chapter by Paulino *et al.* (2003). FGM may exhibit isotropic or anisotropic material properties depending on the processing technique and the practical engineering requirements. In the present paper, anisotropic material properties of FGM are considered since isotropic FGM have been investigated by several authors previously, see e.g., Erdogan (1995), Sladek *et al.* (2000), Rao and Rahman (2003), Kim and Paulino (2002), Dolbow and Gosz (2002), and Yue *et al.* (2003).

Cracking of structures is an important phenomenon in many engineering applications. The use of linear elastic fracture mechanics to predict the crack behaviour in elastic solids under different loading conditions is well established in engineering applications. In conventional linear elastic fracture mechanics analysis in two dimensions, the primary focus is on the Stress Intensity Factors (SIF), K_I and K_{II}, which characterise the near-tip stress fields. A number of studies performed over the years have suggested the need to consider leading non-singular term in the Williams' series expansion in order to offer better predictions of the crack path direction and the stability (Cotterell and Rice, 1980), and fracture toughness in elastic solids under conditions of low crack tip stress triaxiality (Williams and Ewing, 1972; Sumpter, 1993; Betegon and Hancock, 1991; Sumpter and Hancock, 1991). This leading non-singular term is often referred to in the literature as the T-stress. It represents the stress acting parallel to the crack plane. Both crack parameters, the stress intensity factor and the T-stress, are important for a more precise characterisation of crack fields in the crack tip vicinity. Accurate computational methods for their evaluation are thus needed. Many efficient techniques for evaluation of these fracture parameters in homogeneous solids exist in the literature. However, due to the high mathematical complexity of the boundary or initial-boundary value problem, most investigations on cracked FGM known in the literature are restricted to isotropic materials (Noda and Jin, 1993a,b; Jin and Noda, 1993a,b; Nemat-Alla and Noda, 1996). Gu and Asaro (1997) studied orthotropic FGM considering a four-point bending specimen with varying Young's modulus and varying Poisson's ratio. Ozturk and Erdogan (1997, 1999) used the singular integral equation method to investigate mode I and mixed-mode crack problems in an infinite nonhomogeneous orthotropic medium, with a crack aligned to one of the principal material axes and a constant Poisson's ratio. Recently, Kim and Paulino (2003b) have proposed the domain interac-

tion integral method for the evaluation of stress intensity factors in orthotropic, functionally graded materials. Less attention is devoted to the evaluation of the T-stress. Larsson and Carlsson (1973), Leevers and Radon (1982), Kfouri (1986), Sherry *et al.* (1995), Nakamura and Parks (1992), Olsen (1994), J. and V. Sladek (1997a,b), Sladek *et al.* (1997), Smith *et al.* (2001), Kim and Paulino (2003a), and Shah *et al.* (2005) are among the authors who have investigated the T-stress but their works were restricted to homogeneous bodies. Recently Kim and Paulino (2004) presented a computational method for the evaluation of the T-stress in orthotropic, functionally graded materials under a static load. The method is based on the interaction integral expressed by a domain integral. It requires an accurate evaluation of quantities occurring in the domain integral at the crack tip vicinity. It is well known that the accuracy of the computed stress and displacement fields at the crack tip vicinity is lower than for those located far away from the crack tip. Therefore, a contour-domain integral formulation for the evaluation of stress intensity factors and T-stresses in orthotropic FGM under thermal and mechanical impact loads is proposed in this paper. Only the inertial term and the term with the gradients of material parameters appear in the domain integral.

The solution of the boundary or initial boundary value problems for continuously nonhomogeneous solids requires advanced numerical methods due to the high mathematical complexity. Beside the well-established Finite Element Method (FEM), the Boundary Element Method (BEM) provides an efficient and popular alternative to the FEM for solving certain classes of boundary or initial boundary value problems (Aliabadi, 1997). The conventional BEM is accurate and efficient for many engineering problems. However, it requires the availability of the fundamental solutions or Green's functions to the governing equations. Material anisotropy increases the number of elastic constants in Hooke's law, and hence makes the construction of the fundamental solutions cumbersome. For 2D elastostatic problems in homogeneous, anisotropic and linear elastic solids, the fundamental solution is available in closed form (Eshelby *et al.*, 1953; Schclar, 1994) and it is given in a complex variable space. Closed-form elastostatic fundamental solutions for 3D anisotropic elasticity exist only for special cases, such as for transversally isotropic or cubic materials (Ding *et al.*, 1997). In contrast to the static case, very few applications of the BEM to elastodynamic problems in homogeneous, anisotropic and linear elastic solids can be found in the literature (Wang and Achenbach, 1996; Albuquerque *et al.*, 2002, 2004; Kgl and Gaul, 2000), although the BEM has been successfully applied to elastodynamic problems in homogeneous, isotropic and linear elastic solids for many years. The main reason lies in the elastodynamic fundamental solutions for anisotropic and linear elastic solids,

which cannot be given in simple and closed forms and thus make their numerical implementation somewhat cumbersome. Time-domain elastodynamic fundamental solutions for 2D anisotropic and linear elastic solids have been applied by Wang *et al.* (1996) to transient wave scattering analysis by a cavity. The dual reciprocity BEM has also been used by Albuquerque *et al.* (2002) and Kögl and Gaul (2000), where the corresponding elastostatic fundamental solutions have been utilized.

In this paper, a new computational method is presented to analyze the boundary value problems in anisotropic FGM with cracks. The governing equations for nonhomogeneous, anisotropic and linear elastic solids are more complex than those for the homogeneous counterpart. The material nonhomogeneity gives rise to an additional complication in the derivation of elastostatic and elastodynamic fundamental solutions. For general nonhomogeneous, anisotropic and linear elastic solids, elastostatic and elastodynamic fundamental solutions are, hitherto, to the best of the authors' knowledge, not available. One possibility to obtain a BEM formulation is based on the use of fundamental solutions for a fictitious homogeneous medium (Sladek *et al.*, 1993). This approach, however, leads to a boundary-domain integral formulation with a domain-integral containing the gradients of the primary fields. Owing to the singularities, special care is required in the numerical integration when the standard boundary-domain formulation is employed. Moreover, the system matrix is relatively large and fully populated. To overcome such difficulties, a local integral formulation can be used for general nonhomogeneous solids (Sladek *et al.*, 2000; Mikhailov, 2002). The application of Local Integral Equations (LIE) requires the use of a domain approximation of the physical fields in the numerical implementation.

Meshless formulations have become increasingly popular in recent years due to their higher adaptivity and lower cost for preparing input data in the numerical analysis. Several meshless methods have already been proposed in literature (Belytschko *et al.*, 1994; Atluri and Shen, 2002; Atluri, 2004). Many of them are derived from a weak form formulation on a global domain or a set of local subdomains. The global formulation requires background cells for the integration of the weak form. In contrast, the local weak form formulation needs no cells and therefore, the corresponding methods are often called truly meshless methods. If a simple form for the geometry of the subdomains is chosen, numerical integrations over them can be easily carried out. The Meshless Local Petrov-Galerkin (MLPG) method is a fundamental base for the derivation of many meshless formulations, since trial and test functions can be chosen from different functional spaces. If a unit step function is used as the

test function in the local weak form to derive LIE, the form of LIE is much simpler than that provided by utilizing the singular fundamental solutions. Such an approach has been recently applied to problems in homogeneous, anisotropic and linear elastic solids by Sladek *et al.* (2004). It is extended in this paper to continuously nonhomogeneous, anisotropic and linear elastic solids. It yields a pure contour or boundary integral formulation on local boundaries for static problems in anisotropic linear elasticity. In anisotropic elastodynamics an additional domain-integral containing the inertial terms is involved. The Laplace transform is applied to eliminate the time variable in the governing equations and the boundary conditions of elastodynamic problems. Then, the local boundary integral equations are derived in the Laplace transformed domain. Several quasi-static boundary value problems have to be solved for various values of the Laplace transform parameter. The integral equations have a very simple nonsingular form. Moreover, both the contour and domain integrations can be easily carried out on circular subdomains. The Stehfest's inversion method (Stehfest, 1970) is applied to obtain the time-dependent solutions. The spatial variation of the displacements is approximated by the moving least-squares (MLS) scheme. Several numerical examples for crack problems in nonhomogeneous orthotropic and linear elastic solids are presented and discussed.

2. Evaluation of the first fracture parameter – the SIF

In stationary thermoelasticity for non-homogeneous anisotropic bodies, the thermal and the stress fields are described by the following governing equations (Nowacki, 1975)

$$(\lambda_{ij}\theta_{,j})_{,i} = -Q \qquad \sigma_{ij,j} + X_i = 0 \tag{2.1}$$

where θ is the temperature measured in the scale with its origin at the equilibrium state, X_i and Q are the body force vector and the heat source respectively, and σ_{ij} is the stress tensor. The thermal conductivity tensor λ_{ij} is a continuous function of Cartesian coordinates. A subscript preceded by a comma denotes differentiation with respect to the corresponding Cartesian coordinate.

The strain tensor ε_{ij} is given by the displacement gradients as follows

$$\varepsilon_{ij} = \frac{1}{2}(u_{i,j} + u_{j,i}) \tag{2.2}$$

In the presence of a temperature gradient, the total strain tensor can be decomposed into its elastic part ε_{ij}^e and another one accounting for the free thermal expansion of the medium. Thus,

$$\varepsilon_{ij} = \varepsilon_{ij}^e + \alpha_{ij}\theta \tag{2.3}$$

where α_{ij} is the tensor of thermal expansions.

According to the Neumann hypothesis, the stress tensor is related to the elastic strain in the usual way, viz

$$\sigma_{ij} = c_{ijkl}\varepsilon_{kl}^e \tag{2.4}$$

where c_{ijkl} is the elasticity tensor. For an isotropic continuum, it is given by

$$c_{ijkl} = \mu\Big(\frac{2\nu}{1-2\nu}\delta_{ij}\delta_{kl} + \delta_{ik}\delta_{jl} + \delta_{il}\delta_{jk}\Big) \tag{2.5}$$

where μ is the shear modulus and ν is Poisson's ratio. Note that the material is non-homogeneous in general, since the elasticity tensor and the coefficients of thermal expansions depend on the spatial position.

The elastic strain energy density $W = W(\varepsilon_{ij}, x_i)$ can be written in the following form

$$W = \frac{1}{2}c_{ijkl}(\varepsilon_{ij} - \alpha_{ij}\theta)(\varepsilon_{kl} - \alpha_{kl}\theta) \tag{2.6}$$

Then, the gradient of strain energy density is given as

$$W_{,m} = \frac{\partial W}{\partial \varepsilon_{ij}}\frac{\partial \varepsilon_{ij}}{\partial x_m} + \Big(\frac{\partial W}{\partial x_m}\Big)_{\exp l} = \frac{\partial W}{\partial \varepsilon_{ij}^e}\frac{\partial \varepsilon_{ij}}{\partial x_m} + \Big(\frac{\partial W}{\partial x_m}\Big)_{\exp l} \tag{2.7}$$

where the term for the "explicit" derivative of the strain energy density for non-homogeneous materials becomes

$$\Big(\frac{\partial W}{\partial x_m}\Big)_{\exp l} = \frac{1}{2}c_{ijkl,m}\varepsilon_{ij}^e\varepsilon_{kl}^e - \sigma_{kl}\alpha_{kl,m}\theta - \sigma_{kl}\alpha_{kl}\theta_{,m} \tag{2.8}$$

Utilizing Eqs. (2.2) and (2.4), the gradient of the strain energy density can be rewritten in the form

$$W_{,m} = (\sigma_{ij}u_{i,m})_{,j} - \sigma_{ij,j}u_{i,m} + (W_{,m})_{\exp l} \tag{2.9}$$

Then, from Eqs. (2.9) and $(2.1)_2$, it follows that

$$(W\delta_{jm} - \sigma_{ij}u_{i,m})_{,j} = X_i u_{i,m} + (W_{,m})_{\exp l} \tag{2.10}$$

An integral form of Eq. (2.10) may be obtained upon application of the divergence theorem. If Ω is a regular bounded region enclosed by a surface Γ whose unit outward normal vector is $\boldsymbol{n}$, it follows that

$$\int_{\Gamma}(W\delta_{jm}-\sigma_{ij}u_{i,m})n_j\,d\Gamma=\int_{\Omega}X_iu_{i,m}\,d\Omega+\int_{\Omega}(W_{,m})_{\exp l}\,d\Omega \tag{2.11}$$

The integral identity (2.11) is valid in a region where no field irregularities prevail. In a crack problem, the stresses at the crack tip are singular and the displacements are discontinuous across both crack-surfaces. Therefore, a cut-off along the crack with a small region in the vicinity of a crack tip Ω_ε has to be excluded. This region is surrounded by Γ_ε as shown in Fig. 1. The global Cartesian coordinate system is defined in such a way that the principal axes of orthotropy are aligned with the global coordinates. Both fields σ_{ij} and u_i are regular in the region $\Omega-\Omega_\varepsilon$. The contour $\Gamma=\Gamma_0+\Gamma_c^+-\Gamma_\varepsilon+\Gamma_c^-$ is a closed integration path in the counter-clockwise direction. The radius ε is considered to be very small and shrunk to zero in the limiting process. The crack surfaces Γ_c^+ and Γ_c^- are assumed to be free of tractions, i.e., $t_i=\sigma_{ij}n_j=0$, and the crack is parallel to the x_1-axis of the local Cartesian coordinate system. Then, Eq. (2.11) can be written as

$$\begin{aligned}\int_{\Gamma_\varepsilon}(W\delta_{jm}-\sigma_{ij}u_{i,m})n_j\,d\Gamma&=\int_{\Gamma_0}(W\delta_{jm}-\sigma_{ij}u_{i,m})n_j\,d\Gamma+\\&+\int_{\Gamma_c^+}(W^+-W^-)\delta_{2m}\,d\Gamma-\lim_{\varepsilon\to0}\int_{\Omega-\Omega_\varepsilon}X_iu_{i,m}\,d\Omega-\lim_{\varepsilon\to0}\int_{\Omega-\Omega_\varepsilon}(W_{,m})_{\exp l}\,d\Omega\end{aligned} \tag{2.12}$$

The left-hand side of Eq. (2.12) is identical to the definition of the $\widehat{J}$-integral (Kishimoto *et al.*, 1980) for $m=1$, which has the following form

$$\widehat{J}=\int_{\Gamma_0}(Wn_1-\sigma_{ij}n_ju_{i,1})\,d\Gamma-\lim_{\varepsilon\to0}\int_{\Omega-\Omega_\varepsilon}X_iu_{i,1}\,d\Omega-\lim_{\varepsilon\to0}\int_{\Omega-\Omega_\varepsilon}(W_{,1})_{\exp l}\,d\Omega \tag{2.13}$$

Consider two independent equilibrium states in an orthotropic, functionally graded material. Let the state 1 correspond to the actual state for given boundary conditions, and let the state 2 correspond to an auxiliary state, which can be either the mode I or the mode II near-tip displacement and stress fields. The asymptotic distribution of the stress and the displacement fields in the vicinity of the crack tip in a continuously nonhomogeneous medium is the same as in the homogeneous one. We select the auxiliary stress and

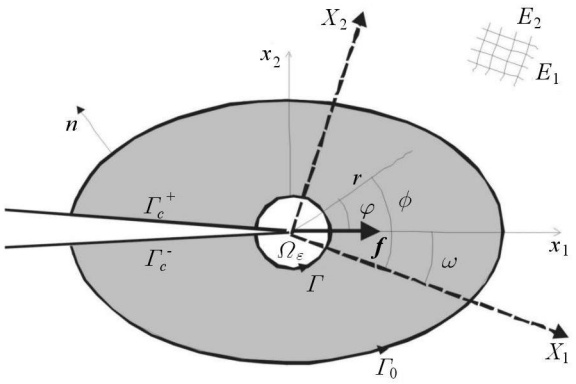

Fig. 1. Integration paths and coordinate definitions

displacement fields, denoted by superscript (2), as the crack tip asymptotic fields in the orthotropic elastic solid given by (Sih *et al.*, 1965)

$$
\begin{aligned}
\sigma_{11}^{(2)} &= \frac{K_I^{(2)}}{\sqrt{2\pi r}}\mathrm{Re}\Big[\frac{\mu_1^{tip}\mu_2^{tip}}{\mu_1^{tip}-\mu_2^{tip}}\Big(\frac{\mu_2^{tip}}{A_2}-\frac{\mu_1^{tip}}{A_1}\Big)\Big]+\\
&+\frac{K_{II}^{(2)}}{\sqrt{2\pi r}}\mathrm{Re}\Big[\frac{1}{\mu_1^{tip}-\mu_2^{tip}}\Big(\frac{(\mu_2^{tip})^2}{A_2}-\frac{(\mu_1^{tip})^2}{A_1}\Big)\Big]\\
\sigma_{22}^{(2)} &= \frac{K_I^{(2)}}{\sqrt{2\pi r}}\mathrm{Re}\Big[\frac{1}{\mu_1^{tip}-\mu_2^{tip}}\Big(\frac{\mu_1^{tip}}{A_2}-\frac{\mu_2^{tip}}{A_1}\Big)\Big]+\\
&+\frac{K_{II}^{(2)}}{\sqrt{2\pi r}}\mathrm{Re}\Big[\frac{1}{\mu_1^{tip}-\mu_2^{tip}}\Big(\frac{1}{A_2}-\frac{1}{A_1}\Big)\Big]\\
\sigma_{12}^{(2)} &= \frac{K_I^{(2)}}{\sqrt{2\pi r}}\mathrm{Re}\Big[\frac{\mu_1^{tip}\mu_2^{tip}}{\mu_1^{tip}-\mu_2^{tip}}\Big(\frac{1}{A_1}-\frac{1}{A_2}\Big)\Big]+\\
&+\frac{K_{II}^{(2)}}{\sqrt{2\pi r}}\mathrm{Re}\Big[\frac{1}{\mu_1^{tip}-\mu_2^{tip}}\Big(\frac{\mu_1^{tip}}{A_1}-\frac{\mu_2^{tip}}{A_2}\Big)\Big] \qquad (2.14)\\
u_1^{(2)} &= K_I^{(2)}\sqrt{\frac{2r}{\pi}}\mathrm{Re}\Big[\frac{1}{\mu_1^{tip}-\mu_2^{tip}}(\mu_1^{tip}P_{12}A_2-\mu_2^{tip}P_{11}A_1\Big)\Big]+\\
&+K_{II}^{(2)}\sqrt{\frac{2r}{\pi}}\mathrm{Re}\Big[\frac{1}{\mu_1^{tip}-\mu_2^{tip}}(P_{12}A_2-P_{11}A_1\Big)\Big]
\end{aligned}
$$

$$u_2^{(2)} = K_I^{(2)}\sqrt{\frac{2r}{\pi}}\mathrm{Re}\Big[\frac{1}{\mu_1^{tip}-\mu_2^{tip}}(\mu_1^{tip}P_{22}A_2 - \mu_2^{tip}P_{21}A_1\Big)\Big] +$$
$$+K_{II}^{(2)}\sqrt{\frac{2r}{\pi}}\mathrm{Re}\Big[\frac{1}{\mu_1^{tip}-\mu_2^{tip}}(P_{22}A_2 - P_{21}A_1\Big)\Big]$$

and

$$A_1 = \sqrt{\cos\varphi + \mu_1^{tip}\sin\varphi} \qquad A_2 = \sqrt{\cos\varphi + \mu_2^{tip}\sin\varphi}$$

where (r,φ) are polar coordinates with the origin at the crack tip and related to the local Cartesian coordinate system (x_1, x_2), Re denotes the real part of a complex function, μ_i^{tip} are material parameters at the crack tip, which are roots of the following characteristic equation in terms of the elastic compliances β_{mn} $(m,n = 1,2 \text{ and } 6)$ of the anisotropic material (Lekhnitskii, 1963)

$$\beta_{11}\mu^4 - 2\beta_{16}\mu^3 + (2\beta_{12} + \beta_{66})\mu^2 - 2\beta_{26}\mu + \beta_{22} = 0 \tag{2.15}$$

and

$$P_{ik} = \begin{bmatrix} \beta_{11}\mu_k^2 + \beta_{12} - \beta_{16}\mu_k \\ \beta_{12}\mu_k + \beta_{22}/\mu_k - \beta_{26} \end{bmatrix} \tag{2.16}$$

The auxiliary stress fields in Eq. (2.14) are in equilibrium in absence of the inertial effects, i.e., $\sigma_{ij,j}^{(2)} = 0$. The auxiliary strain field is chosen as

$$\varepsilon_{ij}^{(2)} = S_{ijkl}(\boldsymbol{x})\sigma_{kl}^{(2)} \tag{2.17}$$

which differs from $S_{ijkl}^{tip}\sigma_{kl}^{(2)}$, where $S_{ijkl}(\boldsymbol{x})$ is the compliance tensor of the actual FGM. Thus, the auxiliary strain field in Eq. (2.17) is incompatible with the symmetric part of the auxiliary displacement gradients (Kim and Paulino, 2003b)

$$\varepsilon_{ij}^{(2)} \neq \frac{1}{2}(u_{i,j}^{(2)} + u_{j,i}^{(2)})$$

Although this incompatibility of the strain field vanishes as the contour shrinks to the crack tip, it gives finite contributions on the contour Γ_0 and the domain $\Omega - \Omega_\varepsilon$.

Superposition of the actual and the auxiliary fields leads to another equilibrium state (state s) for which the J-integral is given as

$$J^{(s)} = \int_{\Gamma_0} \Big[\frac{1}{2}(\sigma_{ij}+\sigma_{ij}^{(2)})(\varepsilon_{ij}+\varepsilon_{ij}^{(2)})n_1 - (\sigma_{ij}+\sigma_{ij}^{(2)})n_j(u_{i,1}+u_{i,1}^{(2)})\Big]\, d\Gamma +$$

$$- \lim_{\varepsilon\to 0} \int_{\Omega-\Omega_\varepsilon} X_i(u_{i,1}+u_{i,1}^{(2)})\, d\Omega - \lim_{\varepsilon\to 0} \int_{\Omega-\Omega_\varepsilon} \frac{1}{2} C_{ijkl,1}(\varepsilon_{kl}+\varepsilon_{kl}^{(2)})(\varepsilon_{ij}+\varepsilon_{ij}^{(2)})\, d\Omega +$$

$$- \lim_{\varepsilon\to 0} \int_{\Omega-\Omega_\varepsilon} (\sigma_{kl}+\sigma_{kl}^{(2)})(\alpha_{kl,1}\theta + \alpha_{kl}\theta_{,1})\, d\Omega \tag{2.18}$$

which is conveniently decomposed into

$$J^{(s)} = J + J^{(2)} + M \tag{2.19}$$

where

$$J^{(2)} = \int_{\Gamma_0} \Big[\frac{1}{2}\sigma_{ij}^{(2)}\varepsilon_{ij}^{(2)}n_1 - \sigma_{ij}^{(2)}n_j u_{i,1}^{(2)}\Big]\, d\Gamma - \lim_{\varepsilon\to 0} \int_{\Omega-\Omega_\varepsilon} \frac{1}{2} C_{ijkl,1}\varepsilon_{kl}^{(2)}\varepsilon_{ij}^{(2)}\, d\Omega \tag{2.20}$$

The interaction integral M is then given by

$$\begin{aligned} M = &\int_{\Gamma_0} \Big[\frac{1}{2}(\sigma_{ij}\varepsilon_{ij}^{(2)} + \sigma_{ij}^{(2)}\varepsilon_{ij})n_1 - (\sigma_{ij}n_j u_{i,1}^{(2)} + \sigma_{ij}^{(2)}n_j u_{i,1})\Big]\, d\Gamma + \\ &- \lim_{\varepsilon\to 0} \int_{\Omega-\Omega_\varepsilon} X_i u_{i,1}^{(2)}\, d\Omega + \\ &- \lim_{\varepsilon\to 0} \int_{\Omega-\Omega_\varepsilon} \Big[\frac{1}{2} C_{ijkl,1}(\varepsilon_{kl}\varepsilon_{ij}^{(2)} + \varepsilon_{kl}^{(2)}\varepsilon_{ij}) - \sigma_{kl}^{(2)}(\alpha_{kl,1}\theta + \alpha_{kl}\theta_{,1})\Big]\, d\Omega \end{aligned} \tag{2.21}$$

Using the following identities

$$\begin{aligned} &\sigma_{ij}\varepsilon_{ij}^{(2)} = \sigma_{ij}S_{ijkl}(\boldsymbol{x})\sigma_{kl}^{(2)} = \varepsilon_{kl}\sigma_{kl}^{(2)} \\ &C_{ijkl,1}\varepsilon_{kl}\varepsilon_{ij}^{(2)} = C_{klij,1}\varepsilon_{kl}\varepsilon_{ij}^{(2)} = C_{ijkl,1}\varepsilon_{ij}\varepsilon_{kl}^{(2)} \end{aligned} \tag{2.22}$$

the M integral can be rewritten in the form

$$\begin{aligned} M = &\int_{\Gamma_0} [\sigma_{ij}\varepsilon_{ij}^{(2)}n_1 - \sigma_{ij}n_j u_{i,1}^{(2)} - \sigma_{ij}^{(2)}n_j u_{i,1}]\, d\Gamma - \lim_{\varepsilon\to 0} \int_{\Omega-\Omega_\varepsilon} X_i u_{i,1}^{(2)}\, d\Omega + \\ &- \lim_{\varepsilon\to 0} \int_{\Omega-\Omega_\varepsilon} [C_{ijkl,1}\varepsilon_{kl}\varepsilon_{ij}^{(2)} - \sigma_{kl}^{(2)}(\alpha_{kl,1}\theta + \alpha_{kl}\theta_{,1})]\, d\Omega \end{aligned} \tag{2.23}$$

For mixed-mode crack problems, the relationship of J-integral and stress intensity factors is given by Kim and Paulino (2003b)

$$J = c_{11}K_I^2 + c_{12}K_IK_{II} + c_{22}K_{II}^2 \tag{2.24}$$

where

$$\begin{aligned} c_{11} &= -\frac{a_{22}^{tip}}{2}\mathrm{Im}\Big(\frac{\mu_1^{tip}+\mu_2^{tip}}{\mu_1^{tip}\mu_2^{tip}}\Big) \\ c_{12} &= -\frac{a_{22}^{tip}}{2}\mathrm{Im}\Big(\frac{1}{\mu_1^{tip}\mu_2^{tip}}\Big) + \frac{a_{22}^{tip}}{2}\mathrm{Im}(\mu_1^{tip}\mu_2^{tip}) \\ c_{22} &= \frac{a_{11}^{tip}}{2}\mathrm{Im}(\mu_1^{tip}+\mu_2^{tip}) \end{aligned} \tag{2.25}$$

For two admissible fields (actual and auxiliary) one obtains

$$\begin{aligned} &J^{(s)} = c_{11}(K_I + K_I^{(2)})^2 + c_{12}(K_I + K_I^{(2)})(K_{II} + K_{II}^{(2)}) + c_{22}(K_{II} + K_{II}^{(2)})^2 = \\ &= J + J^{(2)} + M \end{aligned}$$

where

$$J^{(2)} = c_{11}(K_I^{(2)})^2 + c_{12}K_I^{(2)}K_{II}^{(2)} + c_{22}(K_{II}^{(2)})^2$$

and

$$M = 2c_{11}K_IK_I^{(2)} + c_{12}(K_IK_{II}^{(2)} + K_I^{(2)}K_{II}) + 2c_{22}K_{II}K_{II}^{(2)} \tag{2.26}$$

The mode I and the mode II stress intensity factors are evaluated by solving the system of linear algebraic equations

$$2c_{11}K_I + c_{12}K_{II} = M^I \qquad c_{12}K_I + 2c_{22}K_{II} = M^{II} \tag{2.27}$$

resulting from Eq. (2.26) by taking $K_I^{(2)} = 1$, $K_{II}^{(2)} = 0$ for M^I, and $K_I^{(2)} = 0$, $K_{II}^{(2)} = 1$ for M^{II}, respectively. The values M^I and M^{II} are computed numerically by Eq. (2.23) with an adequate choice of the auxiliary solutions according to Eq. (2.14).

The advantage of the presented method for the computation of stress intensity factors through the M-integral technique is high accuracy, because the contour integral is evaluated at points far away from the crack tip. Numerical errors of computed quantities at the crack tip vicinity in a direct computation of SIF from the asymptotic expansion formulae are hence reduced in this approach. The results are also insensitive to the distance of the evaluation point from the crack tip.

Similarly, one can derive the M-integral representation for elastodynamic problems in continuously nonhomogeneous orthotropic materials. The M integral in this case has the following form

$$M = \int_{\Gamma_0} (\sigma_{ij}\varepsilon_{ij}^{(2)} n_1 - \sigma_{ij} n_j u_{i,1}^{(2)} - \sigma_{ij}^{(2)} n_j u_{i,1})\, d\Gamma - \lim_{\varepsilon\to 0} \int_{\Omega-\Omega_\varepsilon} X_i u_{i,1}^{(2)}\, d\Omega + \\ - \lim_{\varepsilon\to 0} \int_{\Omega-\Omega_\varepsilon} (C_{ijkl,1}\varepsilon_{kl}\varepsilon_{ij}^{(2)} - \rho\ddot{u}_i u_{i,1}^{(2)})\, d\Omega \tag{2.28}$$

It should be remarked that the terms in Eq. (2.23) or (2.28) are given in the local coordinate system with the origin at the crack tip as shown in Fig. 1. Recall that the derived expressions (2.23) and/or (2.28) for the M-integral are related to the local Cartesian coordinate system, where $M_{1(local)} = M$. Due to material orthotropy, it is convenient to perform all the numerical calculations in the global Cartesian coordinate system. Thus, in the numerical computation, the M-integrals (M_1 and M_2) are obtained in global coordinates and then transformed according to the law for the transformation of vector components to get the local component $M_{1(local)}$ or equivalently M.

The transformation is given by Kim and Paulino (2004)

$$M = M_{1(local)} = M_{1(global)} \cos\omega + M_{2(global)} \sin\omega \tag{2.29}$$

where

$$M_{m(global)} = \int_{\Gamma_0} (\sigma_{ij}\varepsilon_{ij}^{(2)} n_m - \sigma_{ij} n_j u_{i,m}^{(2)} - \sigma_{ij}^{(2)} n_j u_{i,m})\, d\Gamma + \\ - \lim_{\varepsilon\to 0} \int_{\Omega-\Omega_\varepsilon} X_i u_{i,m}^{(2)}\, d\Omega - \lim_{\varepsilon\to 0} \int_{\Omega-\Omega_\varepsilon} (C_{ijkl,m}\varepsilon_{kl}\varepsilon_{ij}^{(2)} - \rho\ddot{u}_i u_{i,m}^{(2)})\, d\Omega \tag{2.30}$$

and ω is the angle between the x_1-axes of the local and the global coordinate systems.

3. Evaluation of the second fracture parameter – the T-stress

The T-stress is very frequently considered as the second fracture parameter in fracture mechanics analysis. It is the leading non-singular term in the

Williams' (1957) asymptotic expansion of stresses. The T-stress can be computed directly from the above-mentioned asymptotic expansion of stresses or displacements, if the stress intensity factors and the stress or the displacement values at nodal points close to the crack tip are obtained from a numerical analysis. In the literature, such a method where T-stress is computed from the known stress component σ_{11}, is called the boundary layer method (Sherry *et al.*, 1995). A drawback of this method the sensitivity of the results with respect to the distance of the evaluation point from the crack tip. It is therefore suggested that a method shpuld be adopted in which the T-stress is expressed in terms of the solution at points far away from the crack tip. In the following, an integral representation of the T-stress will be derived for a cracked body analysed in the framework of stationary thermoelasticity.

The stresses and the displacements in the crack tip vicinity of a material with a continuous non-homogeneity have the same singularity and angular distributions as those in a homogeneous material. The displacements and the stresses close to the crack tip can be written in an asymptotic form as (Shah *et al.*, 2005)

$$u_1(r,\varphi) = \frac{K_I}{4}\sqrt{\frac{r}{2\pi}}g_1^I(\varphi,\mu_1^{tip},\mu_2^{tip}) + \frac{K_{II}}{4}\sqrt{\frac{r}{2\pi}}g_1^{II}(\varphi,\mu_1^{tip},\mu_2^{tip}) + a_{11}Tr\cos\varphi \tag{3.1}$$

$$u_2(r,\varphi) = \frac{K_I}{4}\sqrt{\frac{r}{2\pi}}g_2^I(\varphi,\mu_1^{tip},\mu_2^{tip}) + \frac{K_{II}}{4}\sqrt{\frac{r}{2\pi}}g_2^{II}(\varphi,\mu_1^{tip},\mu_2^{tip}) + a_{12}Tr\sin\varphi$$

$$\sigma_{ij}(r,\varphi) = \frac{K_I}{\sqrt{2\pi r}}f_{ij}^I(\varphi,\mu_1^{tip},\mu_2^{tip}) + \frac{K_{II}}{\sqrt{2\pi r}}f_{ij}^{II}(\varphi,\mu_1^{tip},\mu_2^{tip}) + T\delta_{i1}\delta_{j1} \tag{3.2}$$

where the functions $f_{ij}^{I,II}(\varphi,\mu_1^{tip},\mu_2^{tip})$ and $g_i^{I,II}(\varphi,\mu_1^{tip},\mu_2^{tip})$ are given in Eqs. (2.14).

An attempt will be made to find an appropriate auxiliary field to obtain the integral expression of the T-stress. In order to obtain a finite contribution of this term in the interaction integral M given by Eq. (2.23), the stress tensor $\sigma_{ij}^{(2)}$ should be proportional to r^{-1}. However, such auxiliary fields multiplied by the first part of the asymptotic expansion of stresses and displacements, which contain the stress intensity factors, give the singular integrand on Γ_ε. These singular terms have to be eliminated only by the angular variation of the auxiliary fields.

The application of a concentrated point-force f at the crack tip in the plane of the crack will give the stress and the displacement fields which will meet the conditions mentioned above. The auxiliary stress field solution due to a concentrated point-force acting at the crack tip of an anisotropic, ho-

mogeneous, and infinite wedge-shaped beam with a unit thickness is given as (Lekhnitskii, 1963)

$$\sigma_{rr}^{(2)} = \frac{C\cos\phi + D\sin\phi}{rL(\phi)} \qquad \sigma_{\phi\phi}^{(2)} = \sigma_{r\phi}^{(2)} = 0 \tag{3.3}$$

where

$$L(\phi) = \beta_{11}^{tip}\cos^4\phi + (2\beta_{12}^{tip} + \beta_{66}^{tip})\sin^2\phi\cos^2\phi + \beta_{22}^{tip}\sin^4\phi$$

with β_{ij}^{tip} being the material compliances at the crack tip, and the constants C and D may be determined from the equilibrium forces in global coordinate system

$$\begin{aligned} C\int_{-\psi_1}^{\psi_2}\frac{\cos^2\phi}{L(\phi)}\,d\phi + D\int_{-\psi_1}^{\psi_2}\frac{\sin\phi\cos\phi}{L(\phi)}\,d\phi &= -f\cos\omega \\ C\int_{-\psi_1}^{\psi_2}\frac{\sin\phi\cos\phi}{L(\phi)}\,d\phi + D\int_{-\psi_1}^{\psi_2}\frac{\sin^2\phi}{L(\phi)}\,d\phi &= -f\sin\omega \end{aligned} \tag{3.4}$$

In Eq. (3.4), the integration bounds ψ_1 and ψ_2 are given by the angles between the X_1-axis and the lower and upper crack faces, respectively.

The auxiliary strains are defined by using the actual material compliances at the considered point of the non-homogeneous medium as

$$\varepsilon_{rr}^{(2)}(\boldsymbol{x}) = \beta_{11}(\boldsymbol{x})\sigma_{rr}^{(2)} \qquad \varepsilon_{\phi\phi}^{(2)}(\boldsymbol{x}) = \beta_{12}(\boldsymbol{x})\sigma_{rr}^{(2)} \tag{3.5}$$

The auxiliary stress fields in global coordinate system can be expressed as

$$\begin{aligned} \sigma_{11}^{(2)} &= \sigma_{rr}^{(2)}\cos^2\phi = \frac{C\cos\phi + D\sin\phi}{rL(\phi)}\cos^2\phi \\ \sigma_{22}^{(2)} &= \sigma_{rr}^{(2)}\sin^2\phi = \frac{C\cos\phi + D\sin\phi}{rL(\phi)}\sin^2\phi \\ \sigma_{12}^{(2)} &= \sigma_{rr}^{(2)}\sin\phi\cos\phi = \frac{C\cos\phi + D\sin\phi}{rL(\phi)}\sin\phi\cos\phi \end{aligned} \tag{3.6}$$

The displacement derivatives for the auxiliary field derived by Kim and Paulino (2004) are

$$
\begin{aligned}
u_{1,1}^{(2)} &= (\beta_{11}^{tip}\cos^2\phi + \beta_{12}^{tip}\sin^2\phi)\frac{C\cos\phi + D\sin\phi}{rL(\phi)} \\
u_{2,2}^{(2)} &= (\beta_{12}^{tip}\cos^2\phi + \beta_{22}^{tip}\sin^2\phi)\frac{C\cos\phi + D\sin\phi}{rL(\phi)} \\
u_{1,2}^{(2)} &= \frac{CL(\phi)\sin\phi - CH_1(\phi) - DH_2(\phi)}{rL(\phi)} \\
u_{2,1}^{(2)} &= \frac{2\beta_{66}^{tip}(C\cos\phi + D\sin\phi)\sin\phi\cos\phi - CL(\phi)\sin\phi + CH_1(\phi) + DH_2(\phi)}{rL(\phi)}
\end{aligned}
\tag{3.7}
$$

where

$$
\begin{aligned}
H_1(\phi) &= \beta_{11}^{tip}\cos^4\phi\sin\phi + \beta_{12}^{tip}\sin\phi\cos^2\phi - \beta_{22}^{tip}\sin^3\phi\cos^2\phi + \\
&\quad -(\beta_{12}^{tip} + \beta_{66}^{tip})\sin\phi\cos^4\phi \\
H_2(\phi) &= \beta_{11}^{tip}\cos^3\phi + \beta_{12}^{tip}\sin^2\phi\cos\phi
\end{aligned}
$$

As it is seen in the previous section, the auxiliary strain field, which follows from Eq. (3.5), has an incompatibility since $\varepsilon_{ij}^{(2)} \neq (u_{i,j}^{(2)} + u_{j,i}^{(2)})/2$. The interaction integral M given by Eq. (2.23) is path-independent since it is expressed in terms of J-integrals. Thus, the contour can be chosen arbitrarily, say, as a circle with the radius ε, which is shrunk to zero. In such a case one can write

$$
M = \lim_{\varepsilon\to 0}\int_{\Gamma_\varepsilon}(\sigma_{ij}\varepsilon_{ij}^{(2)}n_1 - \sigma_{ij}n_j u_{i,1}^{(2)} - \sigma_{ij}^{(2)}n_j u_{i,1})\,d\Gamma \tag{3.8}
$$

The asymptotic displacements and stresses can be split into singular and non-singular parts as follows

$$
u_i = u_i^s + u_i^T \qquad\qquad \sigma_{ij} = \sigma_{ij}^s + \sigma_{ij}^T \tag{3.9}
$$

where the terms with superscript s contain the stress intensity factors in Eq. (3.2) and superscript T is related to the T-stress term

$$
\sigma_{ij}^T = T\delta_{i1}\delta_{j1} \tag{3.10}
$$

The elastic strains at the crack tip corresponding to the uniform T-stress in thermoelasticity are given as

$$
\begin{aligned}
\varepsilon_{11}^T &= \beta_{11}^{tip}T + \alpha_{11}^{tip}\theta^{tip} \\
u_{i,1}^T &= u_{1,1}^T\delta_{i1} = \varepsilon_{11}^T\delta_{i1} = \beta_{11}^{tip}T\delta_{i1} + \alpha_{11}^{tip}\theta^{tip}\delta_{i1}
\end{aligned}
\tag{3.11}
$$

Thus, the M-integral reduces to

$$M = -\lim_{\varepsilon\to 0}\int_{\Gamma_\varepsilon} \sigma_{ij}^{(2)} n_j u_{i,1}^T \, d\Gamma = -(\beta_{11}^{tip} T + \alpha_{11}^{tip}\theta^{tip}) \lim_{\varepsilon\to 0}\int_{\Gamma_\varepsilon} \sigma_{ij}^{(2)} n_j \, d\Gamma = \\ = (\beta_{11}^{tip} T + \alpha_{11}^{tip}\theta^{tip}) f \tag{3.12}$$

The final result of Eq. (3.12) may be rearranged and take the form

$$T = \frac{M - \alpha_{11}^{tip}\theta^{tip} f}{f\beta_{11}^{tip}} \tag{3.13}$$

The unknown displacements, traction vector and temperature, required along the integration path and within the domain enclosed by the integration contour in Eq. (2.30), can be obtained from a numerical or experimental analysis. In this paper, the meshless local integral equation method is used for this purpose.

4. Meshless local Petrov-Galerkin method in continuously non-homogeneous solids

4.1. Uncoupled thermoelasticity

Let us consider a boundary value problem defined in the stationary uncoupled thermoelasticity for a continuously non-homogeneous anisotropic medium, which in 2D is described by the governing equations (2.1). Since Eqs. (2.1) are uncoupled, they can be solved separately. In the first step we solve the heat conduction equation $(2.1)_1$.

Instead of writing the global weak form for the above governing equation, the MLPG methods construct the weak form over local subdomains such as Ω_s, which is a small region taken for each node inside the global domain (Atluri and Shen, 2002). The local subdomains overlap each other, and cover the whole global domain Ω; they could be of any geometric shape and size. In the present paper, the local subdomains are taken to be of circular shape (Fig. 2). The local weak form of the governing equation $(2.1)_1$ can be written as

$$\int_{\Omega_s} [(\lambda_{ij}(\boldsymbol{x})\theta_{,j}(\boldsymbol{x}))_{,i} + Q(\boldsymbol{x})]\theta^*(\boldsymbol{x}) \, d\Omega = 0 \tag{4.1}$$

where $\theta^*(\boldsymbol{x})$ is a weight (test) function.

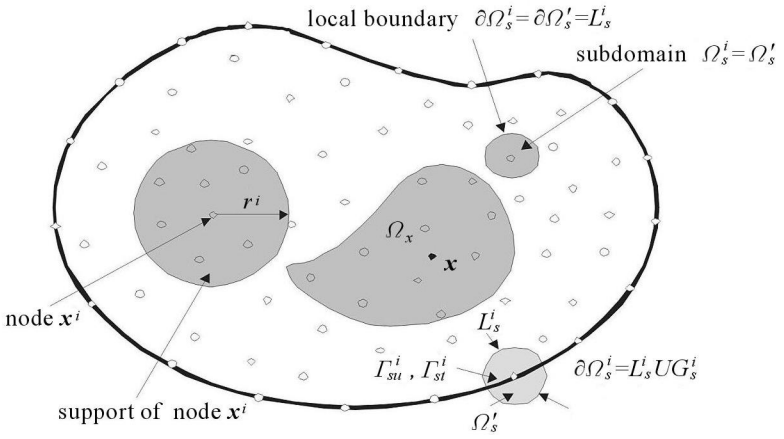

Fig. 2. Local boundaries for weak formulation, the domain Ω_x for MLS approximation of the trial function, and support area of weight function around node $\boldsymbol{x}^i$

Applying the Gauss divergence theorem to Eq. (4.1) one can write

$$\int_{\partial\Omega_s} q(\boldsymbol{x})\theta^*(\boldsymbol{x})\,d\Gamma - \int_{\Omega_s} \lambda_{ij}(\boldsymbol{x})\theta_{,j}(\boldsymbol{x})\theta_{,i}^*(\boldsymbol{x})\,d\Omega + \int_{\Omega_s} Q(\boldsymbol{x})\theta^*(\boldsymbol{x})\,d\Omega = 0 \quad (4.2)$$

where $\partial\Omega_s$ is the boundary of the local subdomain and

$$q(\boldsymbol{x}) = \lambda_{ij}(\boldsymbol{x})\theta_{,j}(\boldsymbol{x})n_i(\boldsymbol{x})$$

The local weak form in Eq. (4.2) is a starting point to derive the local boundary integral equation if an appropriate test function is selected. If a Heaviside step function is chosen as the test function $\theta^*(\boldsymbol{x})$ in each subdomain

$$\theta^*(\boldsymbol{x}) = \begin{cases} 1 & \text{at} \quad \boldsymbol{x} \in \Omega_s \\ 0 & \text{at} \quad \boldsymbol{x} \notin \Omega_s \end{cases}$$

the local weak form, Eq. (4.2), is transformed into a simple local integral equation

$$\int_{\partial\Omega_s} q(\boldsymbol{x})\,d\Gamma = -\int_{\Omega_s} Q(\boldsymbol{x})\,d\Omega \quad (4.3)$$

Equation (4.3) is recognized as the flow balance condition of the subdomain. In the MLPG method, the test and trial functions are not necessarily from the same functional spaces. For internal nodes, the test function is chosen as the

Heaviside step function with the support on the local subdomain. The trial function, on the other hand, is chosen to be the Moving Least-Squares (MLS) interpolation over a number of nodes randomly distributed within the domain of influence. While the local subdomain is defined as the support of the test function on which the integration is carried out, the domain of influence is defined as a region where the weight function is not zero, i.e., all nodes lying inside that region influence the interpolation. The approximate function can be written as (Atluri and Shen, 2002)

$$\theta^h(\boldsymbol{x}) = \boldsymbol{\Phi}^\top(\boldsymbol{x}) \cdot \hat{\boldsymbol{\theta}} = \sum_{a=1}^{n} \phi^a(\boldsymbol{x}) \widehat{\theta}^a \tag{4.4}$$

where $\widehat{\theta}^a$ are fictitious parameters and $\phi^a(\boldsymbol{x})$ is the shape function associated with the node a. The number of nodes n used for the approximation of $\theta(\boldsymbol{x})$ is determined by the weight function $w^a(\boldsymbol{x})$. A spline-type weight function is considered in the present work

$$w^a(\boldsymbol{x}) = \begin{cases} 1 - 6\Big(\dfrac{d^a}{r^a}\Big)^2 + 8\Big(\dfrac{d^a}{r^a}\Big)^3 - 3\Big(\dfrac{d^a}{r^a}\Big)^4 & 0 \leqslant d^a \leqslant r^a \\ 0 & d^a \geqslant r^a \end{cases} \tag{4.5}$$

where $d^a = \|\boldsymbol{x} - \boldsymbol{x}^a\|$ and r^a is the radius of the support domain for the weight function w^a. The directional derivatives of $\theta(\boldsymbol{x})$ are approximated in terms of the same nodal values as

$$\frac{\partial \overline{\theta}^h}{\partial n}(\boldsymbol{x}, p) = n_k(\boldsymbol{x}) \sum_{a=1}^{n} \widehat{\theta}^a(p) \phi^a_{,k}(\boldsymbol{x}) \tag{4.6}$$

Making use of the MLS-approximations (4.4) and (4.6) for $\theta(\boldsymbol{x})$ and

$$q(\boldsymbol{x}) = \lambda_{ij}(\boldsymbol{x}) n_i(\boldsymbol{x}) \sum_{a=1}^{n} \widehat{\theta}^a \phi^a_{,j}(\boldsymbol{x}) \tag{4.7}$$

the local boundary integral equation, Eq. (4.3), for all subdomains yields the following set of equations

$$\sum_{a=1}^{n} \widehat{\theta}^a \int_{\partial\Omega_s} \lambda_{ij}(\boldsymbol{x}) n_j(\boldsymbol{x}) \phi^a_{,j}(\boldsymbol{x}) \, d\Gamma = -\int_{\Omega_s} Q(\boldsymbol{x}) \, d\Omega \tag{4.8}$$

It should be noted that neither the Lagrange multipliers nor penalty parameters are introduced into the local weak form in Eq. (4.1), because the essential

boundary conditions on Γ_θ can be imposed directly using the interpolation approximation in Eq. (4.4)

$$\sum_{a=1}^{n} \phi^a(\boldsymbol{x})\widehat{\theta}^a = \widetilde{\theta}(\boldsymbol{x}) \qquad \text{for } \boldsymbol{x} \in \Gamma_\theta \tag{4.9}$$

The same procedure to derive the local integral equation for the heat conduction equation can be applied to obtain the corresponding LIE for mechanical fields described by Eq. $(2.1)_2$. In the case of elastic materials, the relation between the stress and the strain is given by Hookes law for an anisotropic body

$$\sigma_{ij}(\boldsymbol{x},t) = C_{ijkl}(\boldsymbol{x})\varepsilon_{kl}(\boldsymbol{x},t) = C_{ijkl}(\boldsymbol{x})u_{k,l}(\boldsymbol{x},t) \tag{4.10}$$

where C_{ijkl} is the elasticity tensor which exhibits the symmetries

$$C_{ijkl} = C_{jikl} = C_{klij}$$

The Cauchy formula has been employed for strains in the last equality in Eq. (4.10). Then, the traction vector $t_i = \sigma_{ij}n_j$ is given by

$$t_i(\boldsymbol{x},t) = C_{ijkl}(\boldsymbol{x})u_{k,l}(\boldsymbol{x},t)n_j(\boldsymbol{x}) \tag{4.11}$$

where n_j denotes a unit outward normal vector.

For the plane stress problem of orthotropic materials, one can write

$$\begin{bmatrix} \sigma_{11} \\ \sigma_{22} \\ \sigma_{12} \end{bmatrix} = \mathbf{D}(\boldsymbol{x}) \begin{bmatrix} \varepsilon_{11} \\ \varepsilon_{22} \\ 2\varepsilon_{12} \end{bmatrix} \tag{4.12}$$

where

$$\mathbf{D}(\boldsymbol{x}) = \begin{bmatrix} E_1/e & E_2\nu_{12}/e & 0 \\ E_2\nu_{12}/e & E_2/e & 0 \\ 0 & 0 & G_{12} \end{bmatrix} \qquad \text{with} \qquad e = 1 - \frac{E_2}{E_1}(\nu_{12})^2$$

The local weak form of the governing equation $(2.1)_2$ can be written as

$$\int_{\Omega_s} [\sigma_{ij,j}(\boldsymbol{x}) + X_i(\boldsymbol{x})]u^*_{ik}(\boldsymbol{x})\, d\Omega = 0 \tag{4.13}$$

where $u^*_{ik}(\boldsymbol{x})$ is a test function.

Using the same procedure as for the above thermal analysis, and assuming the test function as

$$u_{ik}^{*}(\boldsymbol{x}) = \begin{cases} \delta_{ik} & \text{at} \quad \boldsymbol{x} \in (\Omega_s \cup \partial\Omega_s) \\ 0 & \text{at} \quad \boldsymbol{x} \notin \Omega_s \end{cases}$$

the local weak form, Eq. (4.13), leads to the local boundary integral equations

$$\int\limits_{\partial\Omega_s} t_i(\boldsymbol{x})\, d\Gamma + \int\limits_{\Omega_s} X_i(\boldsymbol{x})\, d\Omega = 0 \tag{4.14}$$

Note here that a pure contour integral formulation is obtained under the assumption of vanishing body forces. Analogous to the approximation for the temperature, one can approximate the displacements by

$$\boldsymbol{u}^h(\boldsymbol{x}) = \boldsymbol{\Phi}^{\top}(\boldsymbol{x}) \cdot \widehat{\boldsymbol{u}} = \sum_{a=1}^{n} \phi^a(\boldsymbol{x}) \widehat{\boldsymbol{u}}^a \tag{4.15}$$

where the nodal values $\widehat{\boldsymbol{u}}^a$ are fictitious nodal parameters for displacements.

The traction vectors $t_i(\boldsymbol{x})$ at a boundary point $\boldsymbol{x} \in \partial\Omega_s$ are approximated in terms of the same nodal values $\widehat{\boldsymbol{u}}^a$ as

$$\boldsymbol{t}^h(\boldsymbol{x}) = \mathbf{N}(\boldsymbol{x})\mathbf{D} \sum_{a=1}^{n} \mathbf{B}^a(\boldsymbol{x}) \widehat{\boldsymbol{u}}^a \tag{4.16}$$

where the matrix $\mathbf{N}(\boldsymbol{x})$ is related to the normal vector $\boldsymbol{n}(\boldsymbol{x})$ on $\partial\Omega_s$ by

$$\mathbf{N}(\boldsymbol{x}) = \begin{bmatrix} n_1 & 0 & n_2 \\ 0 & n_2 & n_1 \end{bmatrix}$$

and the matrix $\mathbf{B}^a$ is represented by the gradients of the shape functions as

$$\mathbf{B}^a = \begin{bmatrix} \phi^a_{,1} & 0 \\ 0 & \phi^a_{,2} \\ \phi^a_{,2} & \phi^a_{,1} \end{bmatrix}$$

Satisfying the boundary conditions at those nodal points on the global boundary, where displacements are prescribed, and making use of the approximation (4.15), one obtains the discretized form of the displacement boundary conditions given as

$$\sum_{a=1}^{n} \phi^a(\boldsymbol{\zeta}) \widehat{\boldsymbol{u}}^a = \widetilde{\boldsymbol{u}}(\boldsymbol{\zeta}) \qquad \text{for} \quad \boldsymbol{\zeta} \in \Gamma_u \tag{4.17}$$

With the MLS-approximations, Eqs.(4.15) and (4.16) for the unknown fields in the local boundary integral equations (4.14), we obtain the discretized LIE

$$\sum_{a=1}^{n} \widehat{\boldsymbol{u}}^a \int\limits_{L_s+\Gamma_{su}} \mathbf{N}(\boldsymbol{x})\mathbf{D}(\boldsymbol{x})\mathbf{B}^a(\boldsymbol{x})\, d\Gamma = -\int\limits_{\Gamma_{st}} \widetilde{\boldsymbol{t}}(\boldsymbol{x})\, d\Gamma - \int\limits_{\Omega_s} \boldsymbol{X}(\boldsymbol{x})\, d\Omega \tag{4.18}$$

which are considered on the sub-domains adjacent to interior nodes as well as to the boundary nodes on Γ_{st}.

4.2. Elastodynamics

Now, we consider a linear elastodynamic problem in an anisotropic, continuously nonhomogeneous and linear elastic domain Ω bounded by the boundary Γ. The governing equations can be expressed as

$$\sigma_{ij,j}(\boldsymbol{x},t) - \rho(\boldsymbol{x})\ddot{u}_i(\boldsymbol{x},t) = -X_i(\boldsymbol{x},t) \tag{4.19}$$

where ρ is the mass density, and double dots indicate the second derivative with respect to time. The following boundary and initial conditions are assumed

$$\left.\begin{array}{llll} u_i(\boldsymbol{x},t) = \widetilde{u}_i(\boldsymbol{x},t) & \text{on} \quad \Gamma_u & u_i(\boldsymbol{x},t)\big|_{t=0} = u_i(\boldsymbol{x},0) \\ t_i(\boldsymbol{x},t) = \widetilde{t}_i(\boldsymbol{x},t) & \text{on} \quad \Gamma_t & \dot{u}_i(\boldsymbol{x},t)\big|_{t=0} = \dot{u}_i(x,0) \end{array}\right\} \quad \text{in } \Omega$$

where Γ_u and Γ_t are the parts of the global boundary with prescribed displacements and tractions, respectively.

Applying the Laplace transform to the governing equations, Eq. (4.19), we obtain

$$\overline{\sigma}_{ij,j}(\boldsymbol{x},p) - \rho(\boldsymbol{x})p^2\overline{u}_i(\boldsymbol{x},p) = -\overline{F}_i(\boldsymbol{x},p) \tag{4.20}$$

where p is the Laplace transform parameter, and

$$\overline{F}_i(\boldsymbol{x},p) = \overline{X}_i(\boldsymbol{x},p) + pu_i(\boldsymbol{x},0) + \dot{u}_i(\boldsymbol{x},0)$$

The local weak form of Eq. (4.20) can be written as

$$\int\limits_{\Omega_s} [\overline{\sigma}_{ij,j}(\boldsymbol{x},p) - \rho p^2\overline{u}_i(\boldsymbol{x},p) + \overline{F}_i(\boldsymbol{x},p)]u^*_{ik}(\boldsymbol{x})\, d\Omega = 0 \tag{4.21}$$

Using the same procedure as for the uncoupled thermoelasticity discussed above, one obtains the local integral equations

$$\int\limits_{L_s+\Gamma_{su}} \overline{t}_i(\boldsymbol{x},p)\, d\Gamma - \int\limits_{\Omega_s} \rho p^2\overline{u}_i(\boldsymbol{x},p)\, d\Omega = -\int\limits_{\Gamma_{st}} \widetilde{\overline{t}}_i(\boldsymbol{x},p)\, d\Gamma - \int\limits_{\Omega_s} \overline{F}_i(\boldsymbol{x},p)\, d\Omega \tag{4.22}$$

Equation (4.22) is recognized as the overall equilibrium of forces including the inertial ones acting on the subdomain. The approximate Laplace transforms of the displacements can be written as

$$\overline{\boldsymbol{u}}^h(\boldsymbol{x},p) = \boldsymbol{\Phi}^\top(\boldsymbol{x}) \cdot \widehat{\boldsymbol{u}}(p) = \sum_{a=1}^{n} \phi^a(\boldsymbol{x}) \widehat{\boldsymbol{u}}^a(p) \tag{4.23}$$

Similarly, the traction vector $\overline{t}_i(\boldsymbol{x},p)$ at a boundary point $\boldsymbol{x} \in \partial\Omega_s$ is approximated in terms of the same nodal values $\widehat{\boldsymbol{u}}^a(p)$ as

$$\overline{\boldsymbol{t}}^h(\boldsymbol{x},p) = \mathbf{N}(\boldsymbol{x})\mathbf{D} \sum_{a=1}^{n} \mathbf{B}^a(\boldsymbol{x}) \widehat{\boldsymbol{u}}^a(p) \tag{4.24}$$

With the MLS approximations (4.23) and (4.24) for the unknown fields in the local boundary integral equations, Eq. (4.22), we obtain the discretized LIE

$$\begin{aligned} &\sum_{a=1}^{n} \widehat{\boldsymbol{u}}^a(p) \Big(\int\limits_{L_s+\Gamma_{su}} \mathbf{N}(\boldsymbol{x})\mathbf{D}(\boldsymbol{x})\mathbf{B}^a(\boldsymbol{x})\, d\Gamma - \rho p^2 \int\limits_{\Omega_s} \phi^a(\boldsymbol{x})\, d\Omega \Big) = \\ &= - \int\limits_{\Gamma_{st}} \widetilde{\overline{\boldsymbol{t}}}(\boldsymbol{x},p)\, d\Gamma - \int\limits_{\Omega_s} \overline{\boldsymbol{F}}(\boldsymbol{x},p)\, d\Omega \end{aligned} \tag{4.25}$$

which are considered on the sub-domains adjacent to the interior nodes as well as to the boundary nodes on Γ_{st}. Collecting the discretized LIE together with the discretized boundary conditions for displacements, we get the complete system of linear algebraic equations for the computation of the nodal unknowns which are the Laplace transforms of fictitious parameters $\widehat{\boldsymbol{u}}^a(p)$. The boundary and domain integrals are evaluated numerically by the Gaussian quadrature formula since both integrands are regular.

The time-dependent values of the transformed variables can be obtained by an inverse transform. There are many inversion methods available for the Laplace transform. As the Laplace transform inversion is an ill-posed problem, small truncation errors can be greatly magnified in the inversion process and lead to poor numerical results. In the present analysis the Stehfest's algorithm (Stehfest, 1970) is used. An approximate value f_a of the inverse $f(t)$ at a specific time t is given by

$$f_a(t) = \frac{\ln 2}{t} \sum_{i=1}^{N} v_i \overline{f}\Big(\frac{\ln 2}{t} i\Big) \tag{4.26}$$

where

$$v_i = (-1)^{i+N/2} \sum_{k=(i+1)/2}^{\min(i,N/2)} \frac{k^{N/2}(2k)!}{(N/2-k)!k!(k-1)!(i-k)!(2k-i)!}$$

The number $N = 10$ with single precision arithmetic has been found to be optimal for obtaining accurate results. It means that at each time t, N boundary value problems for the corresponding Laplace transform parameters $p = (i \ln 2)/t$, with $i = 1, 2, \ldots, N$, need to be solved. If M is the number of the time instants at which the quantity $f(t)$ has to be found, the number of the Laplace transform solutions $\overline{f}(p_j)$ is then $M \times N$.

5. Numerical results

5.1. A finite plate with a central crack

In the first numerical example, a rectangular orthotropic plate with a central crack is analyzed. The plate considered is subjected to a thermal load with different prescribed temperatures at its bottom and top sides, which are constrained in x_2-direction such that it is equivalent to the case with a prescribed strain $\varepsilon_0 = \alpha(x_1)\theta(h)$, as shown in Fig. 3.

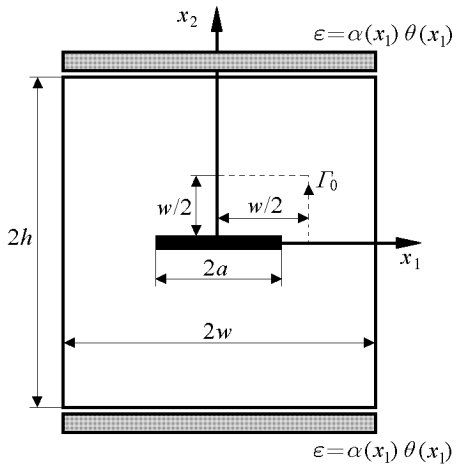

Fig. 3. A finite plate with a center crack parallel to the material gradation

The following geometry is considered: $w = 10\,\mathrm{m}$, $a/w = 0.1$, 0.2, 0.3 and $h = w$. First, isotropic material properties with an exponential variation of

the Young's modulus parallel to the crack line are considered

$$\alpha(\boldsymbol{x}) = \alpha_0 \exp(\delta x_1) \qquad E(x) = E_0 \exp(\gamma x_1) \tag{5.1}$$

with $\alpha_0 = 1.67 \cdot 10^{-5}\,\mathrm{deg}^{-1}$, $E_0 = 10^5\,\mathrm{MPa}$, and a constant Poisson's ratio $\nu = 0.3$. In this case, the temperature distribution is a function of x_2 since the thermal conductivity is considered to be uniform. By virtue of symmetry, only one half of the cracked plate is numerically analyzed. A regular node distribution with $61 \times 30 = 1830$ nodes (61 nodes along each line $x_2 = \mathrm{const}$) is used in our numerical calculations. The integration path Γ_0 for evaluation of the M-integrals has a rectangular shape, as shown in Fig. 3 (dashed line, $5 \times 5\,\mathrm{m}$). To test the accuracy of the proposed method, an additional integration path with a size 20% larger than the dashed line (i.e. $6 \times 6\,\mathrm{m}$) has also been used for evaluating the fracture parameters. The discrepancies of the numerical values obtained for these fracture parameters from the two paths were less than 1%. The stress intensity factors obtained are normalized as $f_I(\pm a) = K_I(\pm a)/[E_0\alpha(a)\theta\sqrt{\pi a}]$. The numerical results of the variations of the normalized stress intensity factor with the crack length at both crack tips in an isotropic FGM with $\gamma = 0.25\,\mathrm{m}^{-1}$ are presented in Fig. 4 for $\delta = 0.1m^{-1}$ and $\delta = -0.1m^{-1}$. The normalized stress intensity factor at the right crack tip increases with increasing crack length; the opposite trend is observed at the left crack tip, however. For an increasing gradation of the thermal expansion with the x_1-coordinate, the normalized stress intensity factor at the right crack tip is also enhanced with respect to the homogeneous case. For a decreasing gradation of the thermal expansion, the normalized stress intensity factor at $x_1 = a$ is reduced, while at $x_1 = -a$, it is enhanced.

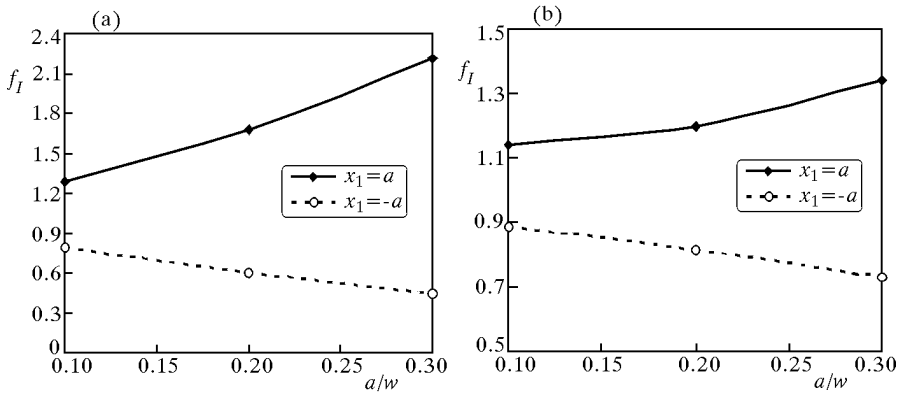

Fig. 4. Variation of stress intensity factors with crack length at both crack tips in an isotropic FGM with $\gamma = 0.25\,\mathrm{m}^{-1}$ and $\delta = 0.1\,\mathrm{m}^{-1}$ (a), and $\delta = -0.1\,\mathrm{m}^{-1}$ (b)

Next, orthotropic material properties with a constant Poisson's ratio $\nu_{12} = 0.3$ and a constant shear modulus $G_{12} = 4 \cdot 10^4$ MPa are considered for the crack problem analyzed above. The Young's moduli are expressed as functions of the parameter $R = E_1/E_2$ with $E_1 = G_{12}(R + 2\nu_{12} + 1)$ and $E_2 = E_1/R$. Two different ratios $R = 0.5$ and $R = 4.5$ are considered in our numerical analyses, and Ei have an exponential variation in the x_i-direction as follows

$$E_i(x) = E_{i0} \exp(\gamma x_1) \tag{5.2}$$

Numerical results for the normalized stress intensity factors $f_I(\pm a) = K_I(\pm a)/[\alpha(a)\theta E_{20}\sqrt{\pi a}]$ are given in Fig. 5. The gradation exponent γ is the same as in the previous isotropic case. One can observe that the orthotropy parameter R has a relatively small influence on the value of the normalized stress intensity factors at both crack tips, at least for the case considered here.

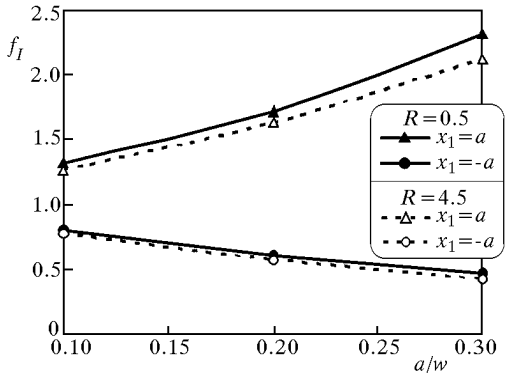

Fig. 5. Variation of stress intensity factors with crack length at both crack tips in an anisotropic FGM with $\delta = 0.1\,\mathrm{m}^{-1}$ and $\gamma = 0.25\,\mathrm{m}^{-1}$

The T-stresses are also analyzed for the same boundary value problem as in the previous examples. First, an isotropic FGM is considered. Variations of the normalized T-stresses $T\sqrt{\pi a}/K_I$ with the crack length at $x_1 = a$ and $x_1 = -a$ are presented in Fig. 6a and Fig. 6b, respectively. The gradation of thermal expansion coefficient has a small influence on T-stress values. With increasing crack length, the absolute value of the T-stresses is reduced, and at both crack tips the T-stresses are almost the same. A much more significant influence of orthotropic properties on the T-stresses is observed in Fig. 7. Increasing the ratio R increases the T-stresses. It is in agreement with the analytical solution for a crack in an infinite plane (Gao and Chiu, 1992) and the FEM results for mechanical loading (Kim and Paulino, 2004).

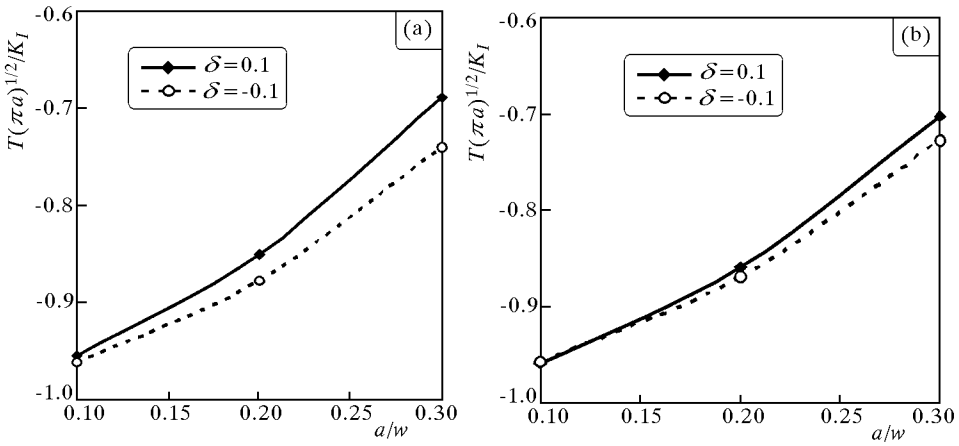

Fig. 6. Variation of T-stress with crack length at the right crack tip $x_1 = a$ (a) and $x_1 = -a$ (b) in an isotropic FGM with $\gamma = 0.25m^{-1}$

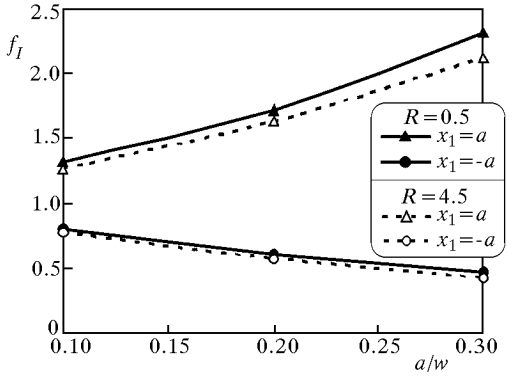

Fig. 7. Variation of T-stress with crack length at both crack tips in an anisotropic FGM with $\delta = 0.1m^{-1}$ and $\gamma = 0.25m^{-1}$

5.2. A finite plate with an edge crack

In the next example, a rectangular orthotropic and linear elastic FGM plate with an edge crack subjected to an impact of mechanical loading is analyzed. The plate length is $2h = 30\,\text{cm}$, the width $w = 10\,\text{cm}$, and the crack length $a/w = 0.4$ (see Fig. 8). At the top and the bottom of the plate, a uniform impact tensile stress $\sigma_{22}(t) = \sigma H(t-0)$ with the Heaviside step time variation is applied. Orthotropic material properties with a constant Poisson's ratio $\nu_{12} = 0.3$, a constant shear modulus $G_{12} = 0.785 \cdot 10^{10}\,\text{N/m}^2$, and a mass density $\rho = 5 \cdot 10^3\,\text{kg/m}^3$ are considered. The Young's moduli E_i have

the same exponential variation (5.2) as in the previous static case. A regular node distribution with 930 nodes is used for the MLS approximation.

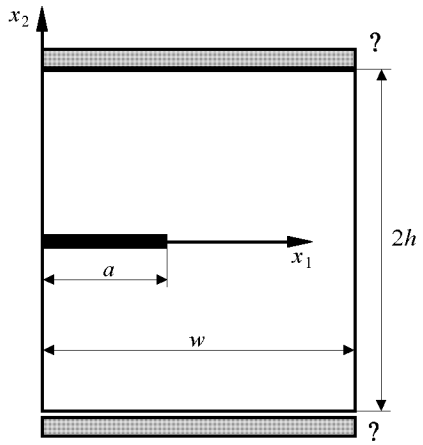

Fig. 8. An edge-cracked orthotropic plate with the material gradation in x_1-direction

The dynamic stress intensity factor is normalized by the static value $K_I^{stat} = \sigma\sqrt{\pi a}$ for convenience. The time variations of the mode I dynamic stress intensity factor are presented in Fig. 9. The gradient parameter γ corresponds to the ratio of Young's moduli $E_{1w}/E_{10} = 5.0$ in the FGM plate. The influence of the material anisotropy, characterized by the parameter $R = E_1/E_2$, on the dynamic stress intensity factor is presented in Fig. 9. The numerical results for the corresponding isotropic case have been obtained by Sladek *et al.* (2005). It can be seen that if the Young's modulus in the x_1-direction is lower than in the direction perpendicular to the crack line, e.g. $R = 0.5$, the wave velocity in the x_1-direction is lower too, and the peak values of the normalized mode I dynamic stress intensity factor are reached at larger time instants than in the isotropic case $R = 1.0$. For $R > 1.0$ the effect of the material anisotropy on the position of the peak $K_I(t)$-values is expected to be opposite.

The time variation of the normalized T-stress T/T_0 is given in Fig. 10, where the corresponding static equivalent is $T_0/\sigma = -0.32$ for the isotropic case. In this case the time variations for the SIF and the T-stresses are very similar. On the basis of the asymptotic expansion of stresses, one can say that the time variation of the stress component σ_{22} ahead of a crack tip follows that of σ_{11} at a small distance behind a crack tip for the considered boundary value problem. For the orthotropic plate with the ratio $R = 0.5$, the T-stress is lower than that for an isotropic plate. The position of the peak T-value

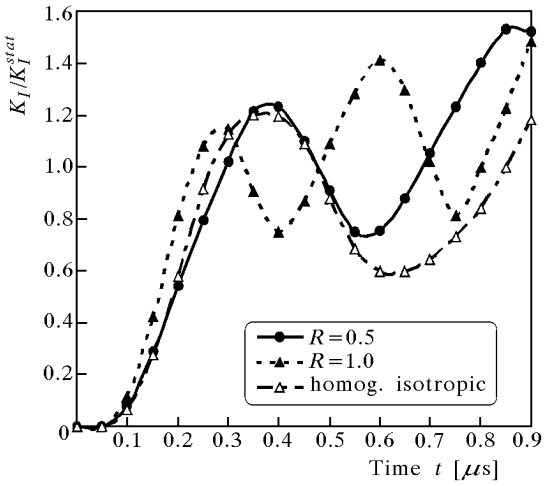

Fig. 9. Normalized mode I dynamic stress intensity factors for an FGM plate with an edge crack

is shifted to larger time instants than in the variation of the stress intensity factor, since the wave propagation velocity in the x_1-direction is reduced. The influence of the material orthotropy on the peak values of the T-stress is more pronounced than that for the stress intensity factors.

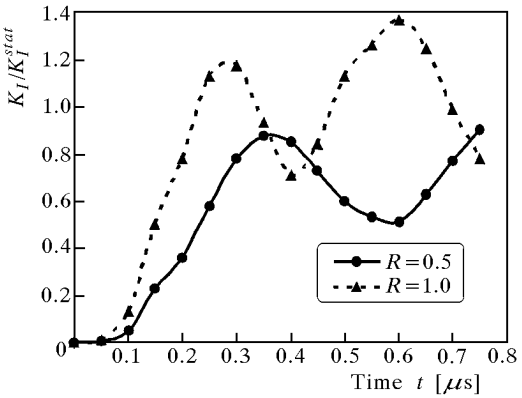

Fig. 10. Time variation of T-stresses for an FGM plate with an edge crack

6. Conclusions

This paper presents efficient numerical methods for the evaluation of stress intensity factors and T-stresses for crack problems in orthotropic, functionally graded materials under thermal and impact mechanical loads. Path-independent integral representations for both fracture parameters are derived. The present integral methods are numerically more expedient than those based on direct computation of the fracture parameters from the asymptotic expansion of the stresses and/or displacements. The integral approach is well suited for elastic meshless analyses. A local boundary integral equation formulation based on the MLPG with a meshless approximation has been successfully implemented to solve 2D boundary and initial-boundary value problems. A unit step function is used as the test function in the local symmetric weak form on the local subdomains. The analyzed domain is divided into small overlapping circular sub-domains on which the local boundary integral equations are applied. The derived local boundary-domain integral equations are non-singular. The proposed method is a truly meshless method, wherein no elements or background cells are involved in either the interpolation or the integration. For elastodynamic crack problems, the Laplace transform technique is implemented. The main difficulty in the application of the classical boundary integral equation formulations for nonhomogeneous, anisotropic and linear elastic solids is the absence of well-established fundamental solutions. This difficulty is circumvented by using the present local integral equation method.

Acknowledgements

The authors acknowledge the supports offered by the Slovak Research and Development Support Agency registered under the project number APVT-20-035404, by the Slovak Grant Agency under the project number VEGA-2/6109/6, by the German Research Foundation (DFG), and the project supported jointly by the German Academic Exchange Service (DAAD) and the Ministry of Education of the Slovak Republic under the project number D/04/25722.

References

1. Albuquerque E.L., Sollero P., Aliabadi M.H., 2002, The boundary element method applied to time dependent problems in anisotropic materials, *Int. Journal Solids and Structures*, **39**, 1405-1422

2. ALBUQUERQUE E.L., SOLLERO P., ALIABADI M.H., 2004, Dual boundary element method for anisotropic dynamic fracture mechanics, *Int. J. Num. Meth. Eng.*, **59** 1187-1205

3. ALIABADI M.H., 1997, Boundary element formulations in fracture mechanics, *Mech. Rev.*, **50**, 83-96

4. AOKI S., KISHIMOTO K., SAKATA M., 1981, Crack tip stress and strain singularity in thermally loaded elastic-plastic materials, *J. Appl. Mech.*, **48**, 428-429

5. ATLURI S.N., SHEN S., 2002, *The Meshless Local Petrov-Galerkin (MLPG) Method*, Techn. Science Press

6. ATLURI S.N., 2004, *The Meshless Local Petrov-Galerkin Method for Domain & BIE Discretizations*, Techn. Science Press

7. BELYTSCHKO T., LU Y., GU L., 1994, Element free Galerkin methods, *Int. J. Num. Meth. Eng.*, **37**, 229-256

8. BETEGON C., HANCOCK J.W., 1991, Two parameter characterization of elastic-plastic crack tip fields, *J. Appl. Mech.*, **58**, 104-110

9. COTTERELL B., RICE J.P., 1980, Slightly curved or kinked cracks, *Int. J. Fracture*, **16**, 155-169

10. DING H., LIANG J., CHEN B., 1997, The unit point force solution for both isotropic and transversaly isotropic media, *Communications in Numerical Methods in Engineering*, **13**, 95-102

11. DOLBOW J., GOSZ M., 2002, On the computation of mixed-mode stress intensity factors in functionally graded materials, *Int. J. Solids Structures*, **39**, 2557-2574

12. ERDOGAN F., 1995, Fracture mechanics of functionally graded materials, *Compos. Eng.*, **5**, 753-770

13. ESHELBY J.D, READ W.T., SHOCKLEY W., 1953, Anisotropic elasticity with applications to dislocations, *Acta Metallurgica*, **1**, 251-259

14. GAO H., CHIU C.H., 1992, Slightly curved or kinked cracks in anisotropic elastic solids, *Int. J. Solids Structures*, **29**, 947-972

15. GU P., ASARO R.J., 1997, Cracks in functionally graded materials, *Int. J. Solids and Structures*, **34**, 1-17

16. JIN Z.H., NODA N., 1993a, Minimization of thermal stress intensity factor for a crack in a metal-ceramic mixture, *Trans. American Ceramic Soc. Functionally Gradient Materials*, **34**, 47-54

17. JIN Z.H., NODA N., 1993b, An internal crack parallel to the boundary of a nonhomogeneous half plane under thermal loading, *Int. J. Eng. Sci.*, **31**, 793–806.

18. JIN Z.H., NODA N., 1994, Crack tip singular fields in nonhomogeneous materials, *J. Appl. Mech.*, **64**, 738-739

19. KFOURI A.P., 1986, Some evaluations of the elastic T-term using Eshelby's method, *Int. J. Fracture*, **30**, 301-315

20. KIM J.H., PAULINO G.H., 2002, Finite element evaluation of mixed mode stress intensity factors in functionally graded materials, *Int. J. Num. Meth. Eng.*, **53**, 1903-1935

21. KIM J.H., PAULINO G.H., 2003a, T-stress, mixed mode stress intensity factors, and crack initiation angles in functionally graded materials: A unified approach using the interaction integral method, *Computer Meth. Appl. Mech. Eng.*, **192**, 1463-1494

22. KIM J.H., PAULINO G.H., 2003b, The interaction integral for fracture of orthotropic functionally graded materials: Evaluation of stress intensity factors, *Int. J. Solids and Structures*, **40**, 3967-4001

23. KIM J.H., PAULINO G.H., 2004, T-stress in orthotropic functionally graded materials: Lekhnitskii and Stroh formalisms, *Int. J. Fracture*, **126**, 345-384

24. KISHIMOTO K., AOKI S., SAKATA M., 1980, On the path independent integral-$\widehat{J}$, *J. Eng. Fracture Mech.*, **13**, 841-850

25. KÖGL M., GAUL L., 2000, A 3-D boundary element method for dynamic analysis of anisotropic elastic solids, *CMES: Computer Modeling in Eng. and Sciences*, **1**, 27-43

26. LARSSON S.G., CARLSSON A.J., 1973, Influence of nonsingular stress terms and specimen geometry on small-scale yielding at crack tips in elastic-plastic materials, *J. Mech. Phys. Solids*, **21**, 263-277

27. LEKHNITSKII S.G., 1963, *Theory of Elasticity of an Anisotropic Body*, Holden Day

28. LEEVERS P.S., RADON J.C., 1982, Inherent stress biaxiality in various fracture specimen geometries, *Int. J. Fracture*, **19**, 311-325

29. MIKHAILOV S.E., 2002, Localized boundary-domain integral formulations for problems with variable coefficients, *Eng. Analysis with Boundary Elements*, **26**, 681-690

30. NAKAMURA T., PARKS D.M., 1982, Determination of elastic T-stresses along three-dimensional crack fronts using an interaction integral, *Int. J. Solids Structures*, **29**, 1597-1611

31. NEMAT-ALLA M., NODA N., 1996, Thermal stress intensity factor for functionally gradient half space with an edge crack under thermal load, *Archive Appl. Mech.*, **66**, 569-580

32. NODA N., JIN Z.H., 1993a, Thermal stress intensity factors for a crack in a functionally gradient material, *Int. J. Solids Structures*, **30**, 1039-1056

33. NODA N., JIN Z.H., 1993b, Steady thermal stresses in an infinite nonhomogeneous elastic solid containing a crack, *J. Thermal Stresses*, **16**, 181-196

34. NODA N., JIN Z.H., 1995, Crack tip singularity fields in non-homogeneous body under thermal stress fields, *JSME Int. Jour. Ser. A*, **38**, 364-369

35. NOWACKI W., 1975, *Dynamic Problems of Thermoelasticity*, PWN, Warsaw

36. OLSEN P.C., 1994, Determining the stress intensity factors K_I, K_{II} and the T-term via the conservation laws using the boundary element method, *Eng. Fracture Mech.*, **49**, 49-60

37. OZTURK M., ERDOGAN F., 1997, Mode I crack problem in an inhomogeneous orthotropic medium, *Int. J. Eng. Sci.*, **35**, 869-883

38. OZTURK M., ERDOGAN F., 1999, The mixed mode crack problem in an inhomogeneous orthotropic medium, *Int. J. Fracture*, **98**, 243-261

39. PAULINO G.H., JIN Z.H., DODDS R.H., 2003, Failure of functionally graded materials, In: *Comprehensive Structural Integrity*, Vol. 2, Karihaloo B., Knauss W.G. (edit.), Elsevier Science, 607-644

40. PAULINO G.H., KIM J.H., 2004, A new approach to compute T-stress in functionally graded materials by means the interaction integral method, *Eng. Fracture Mechanics*, **71**, 1907-1950

41. RAO B.N., RAHMAN S., 2003, Mesh-free analysis of cracks in isotropic functionally graded materials, *Eng. Fracture Mechanics*, **70**, 1-27

42. SCHCLAR S.N., 1994, *Anisotropic Analysis Using Boundary Elements*, Computational Mechanics Publications

43. SHAH P.D., TAN C.L., WANG X., 2005, T-stress solutions for two-dimensional crack problems in anisotropic elasticity using the boundary element method, *Fatigue Fract. Eng. Mater. Struc.*, accepted for publication

44. SHERRY A.H., FRANCE C.C., GOLDTHORPE M.R., 1995, Compendium of T-stress solutions for two and three dimensional cracked geometries, *Fatigue Fract. Eng. Mater. Struct.*, **18**, 141-155

45. SIH G.C., PARIS P.C., IRWIN G.R., 1965, On cracks in rectilinearly anisotropic bodies, *Int. J. Fracture Mechanics*, **1**, 189-203

46. SLADEK V., SLADEK J., MARKECHOVA I., 1993, An advanced boundary element method for elasticity problems in nonhomogeneous media, *Acta Mechanica*, **97**, 71-90

47. SLADEK J., SLADEK V., 1997a, Evaluations of the T-stress for interface cracks by the boundary element method, *Eng. Fracture Mech.*, **56**, 813-825

48. SLADEK J., SLADEK V., 1997b, Evaluation of T-stresses and stress intensity factors in stationary thermoelasticity by the conservation integral method, *Int. J. Fracture*, **86**, 199-219

49. SLADEK J., SLADEK V., FEDELINSKI P., 1997, Integral formulation for elastodynamic T-stresses, *Int. J. Fracture*, **84**, 103-116

50. SLADEK J., SLADEK V., ATLURI S.N., 2000, Local boundary integral equation (LBIE) method for solving problems of elasticity with nonhomogeneous material properties, *Computational Mechanics*, **24**, 456-462

51. SLADEK J., SLADEK V., VAN KEER R., 2003a, Meshless local boundary integral equation method for 2D elastodynamic problems, *Int. J. Num. Meth. Eng.*, **57**, 235-249

52. SLADEK J., SLADEK V., ZHANG CH., 2003b, Application of meshless local Petrov-Galerkin (MLPG) method to elastodynamic problems in continuously nonhomogeneous solids, *CMES: Computer Modeling in Eng. & Sciences*, **4**, 637-648

53. SLADEK J., SLADEK V., ATLURI S.N., 2004, Meshless local Petrov-Galerkin method in anisotropic elasticity, *CMES: Computer Modeling in Eng. & Sciences*, **6**, 477-489

54. SLADEK J., SLADEK V., ZHANG CH., 2005, An advanced numerical method for computing elastodynamic fracture parameters in functionally graded materials, *Computational Materials Science*, **32**, 532-543

55. SMITH D.J., AYATOLLAHI M.R., PAVIER M.J., 2001, The role of T-stress in brittle fracture for linear elastic materials under mixed-mode loading, *Fatigue Fracture Eng. Material Structure*, **24**, 137-150

56. STEHFEST H., 1970, Algorithm 368: numerical inversion of Laplace transform, *Comm. Assoc. Comput. Mech.*, **13**, 47-49

57. SUMPTER J.D.G., 1993, An experimental investigation of the T-stress approach, In: *Constraint Effects in Fracture, ASTM STP*, **1171**, 429-508

58. SUMPTER J.D.G., HANCOCK J.W., 1991, Shallow crack toughness of HY80 welds – an analysis based on T, *Int. J. Press. Vess. Piping*, **45**, 207-229

59. SURESH S., MORTENSEN A., 1998, *Fundamentals of Functionally Graded Materials*, Institute of Materials, London

60. YUE Z.Q., XIAO H.T., THAM L.G., 2003, Boundary element analysis of crack problems in functionally graded materials, *Int. J. Solids and Structures*, **40**, 3273-3291

61. WANG C.Y., ACHENBACH J.D., 1996, Two dimensional time domain BEM for scattering of elastic waves in solids of general anisotropy, *Int. Journal of Solids and Structures*, **33**, 3843-3864

62. WILLIAMS M.L., 1957, On the stress distribution at the base of stationary crack, *J. Appl. Mech.*, **24**, 109-114

63. WILLIAMS J.G., EWING P.D., 1972, Fracture under complex stress – the angled crack problem, *J. Fracture Mech.*, **8**, 441-446

Wyznaczanie parametrów pękania dla szczelin w materiałach funkcjonalnie gradientowych metodą bezsiatkową

Streszczenie

Przedstawiono bezsiatkową metodę analizy szczelin opartą na podejściu Petrova-Galerkina dla dwuwymiarowych liniowo-sprężystych i anizotropowych ośrodków o zmieniających się własnościach materiałowych. Rozważono zarówno kwazistatyczne problemy naprężeń cieplnych, jak i zagadnienia elastodynamiki, w których zastosowano aparat transformacji Laplace'a. Badany obszar podzielono na małe podobszary kołowe. Jako funkcję testową w lokalnej, słabej postaci zastosowano jednostkową funkcję schodkową, co prowadzi do lokalnych równań całkowych (LIE). Metodę ruchomych najmniejszych kwadratów (MLS) zastosowano do przybliżenia wielkości fizycznych w LIE. Przedstawiono efektywne metody numeryczne wyznaczania parametrów pękania, a w szczególności współczynników koncentracji naprężeń oraz naprężeń T dla szczelin w materiałach funkcjonalnie gradientowych (FGM). Przedstawiono niezależne od drogi całkowania reprezentacje tych parametrów w materiałach FGM o kontynualnie zmieniającej się niejednorodności.

Manuscript received January 4, 2006; accepted for print April 4, 2006